Université de Mons
Faculté Polytechnique – Service de Mécanique Rationnelle, Dynamique et Vibrations
31, Bld Dolez - B-7000 MONS (Belgique)
065/37 42 15 – georges.kouroussis@umons.ac.be

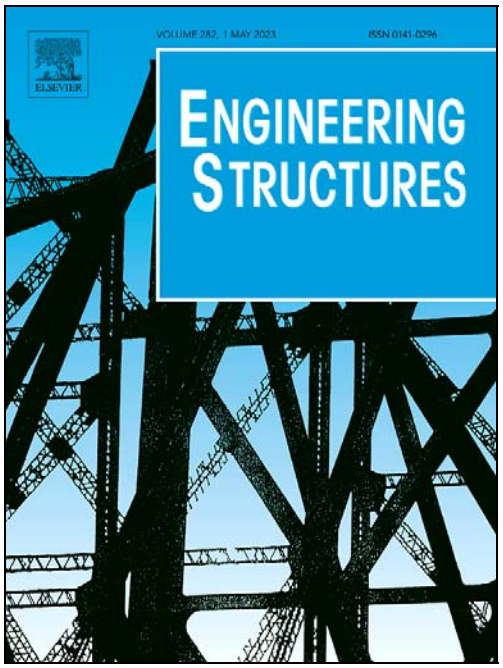

S. Ouakka, A. Gueddida, Y. Pennec, B. Djafari-Rouhani, G. Kouroussis, O. Verlinden,
Efficient mitigation of railway induced vibrations using seismic metamaterials,
Engineering Structures, 284: 115767, 2023.

Engineering Structures 284 (2023) 115767

Contents lists available at ScienceDirect

Engineering Structures

journal homepage: www.elsevier.com/locate/engstruct

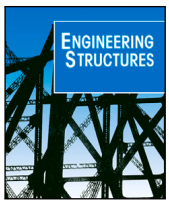

Efficient mitigation of railway induced vibrations using seismic metamaterials

Slimane Ouakka [a,*], Abdellatif Gueddida [b], Yan Pennec [b], Bahram Djafari-Rouhani [b], Georges Kouroussis [a], Olivier Verlinden [a]

[a] Department of Theoretical Mechanics, Dynamics and Vibrations, Faculty of Engineering, University of Mons, Mons, Belgium
[b] Institut d'Electronique, Microélectronique et Nanotechnologie, UMR CNRS 8520, Université de Lille, 59650 Villeneuve d'Ascq, France

ARTICLE INFO

Keywords:
Ground-borne vibration and noise attenuation
Train–track–soil interactions
Seismic metamaterials
Light Rail Vehicle
Metamaterials band gap
Railway mitigation measure
Periodic barriers

ABSTRACT

The fast growth of railway transport pushed by its sustainability requires all railway stakeholders to work together to minimise any possible drawbacks that might slow down this positive trend. Among these, the induced vibrations generated at the wheel–rail interaction during train passage are the most significant, especially in urban areas where in the form of ground-borne vibrations and/or noise negatively affects the daily life of the residents. In this direction, the innovative concept of seismic metamaterial can enhance the vibration attenuation levels of existing mitigation measures and, at the same time, ensure a straightforward application in the railway environment. This paper uses a combined vehicle/track/soil prediction dynamic model of the T2000 LRV (Light Rail Vehicle) tram operating in Brussels, based on a two-step approach already validated in the past, to analyse the effects that the inclusion of seismic metamaterials within the transmission path has in terms of vibration attenuation. In particular, a four-by-four group of piles is examined with different material proprieties for the inclusions, considering a range of velocities and distances from the track in order to quantify the achievable Insertion Loss (IL) for each configuration depending on the distances and the tram speed, attaining ILs up to 10 [dB]. The study is then extended to other possible arrangements of the group of piles, providing a direct relationship between the repetitiveness of each row of the primitive unit cell of the metamaterial and the gained levels of attenuation, in order to give a base for the costs of this type of mitigation measure. Furthermore, the influence on the attenuation levels of the soil characteristics, is evaluated by considering an ideal uniform underground, extending the IL to 18 [dB] in the case of steel inclusion. Finally, the paper gives insights into the use of metamaterials as mitigation measures for railway-induced vibration in order to understand and evaluate the potential of this novel concept and its benefits.

1. Introduction

Modern times are characterised by countries attempting to reduce the carbon footprint of various different industries. In this vein, for the transport industry, the target is to make the railway system the most used means of transportation because of its sustainability and low carbon emissions. This growth has led to a denser network across the globe that, in turn, has increased the frequency and the levels of the induced vibrations generated by the wheel–rail interaction.

The induced vibrations generated at the wheel–rail interface are due to different mechanisms, including track and wheel deformation, dynamic loads and element spacing [1]. The waves created propagate through the soil until they reach the surrounding buildings, and the final effects of their excitation are then perceived by the residents as the feelable movement through the floors and/or noise caused by the structural oscillations, named ground-borne vibrations (in the range 1–100 Hz) and ground-borne noise (in the range 20–250 Hz), as depicted in Fig. 1. Ground-borne vibrations are generally associated with surface railways whereas ground-borne noise is more often associated with trains in tunnels [2]. In addition to the annoyance to building occupants, low-frequency vibration can also cause relevant problems to sensitive equipment [3], whereas the impacts on buildings are mostly cosmetic.

Therefore, it is of relevant interest to develop mitigation measures that can attenuate these vibrations in order to further boost rail transport development. These measures can be applied to all three subsystems of the railway environment. A comprehensive comparison was presented by Ouakka et al. [2,4], highlighting some of the most commonly used mitigation measures:

* Corresponding author.
E-mail address: slimane.ouakka@umons.ac.be (S. Ouakka).

https://doi.org/10.1016/j.engstruct.2023.115767
Received 30 September 2022; Received in revised form 9 January 2023; Accepted 3 February 2023
Available online 20 March 2023

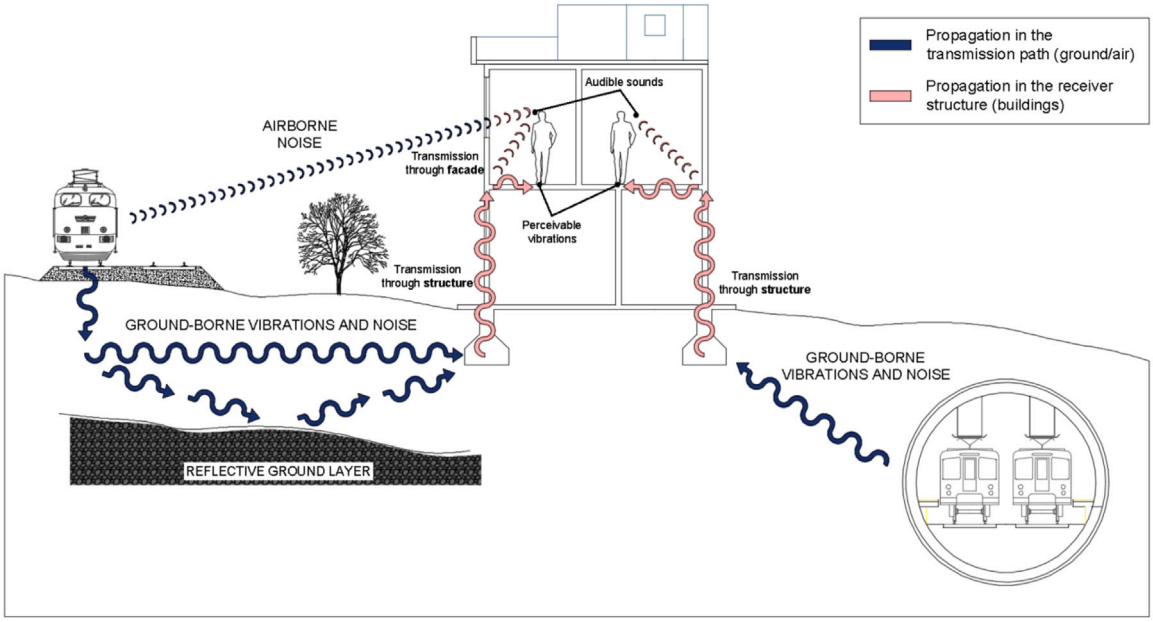

Fig. 1. Surface and underground railway mechanism effects and transmission paths of air-borne noise and ground-borne vibrations and noise [4].

- On the vehicle, improving wheel roundness, reduction of the unsprung mass, reduction of speed and introducing resilient wheels.
- On the track, through rail enhancements, fastener enhancements, sleeper and ballast enhancements and other track technologies.
- On the transmission path, increasing the distance, introducing an embankment, protection barriers, and improvement of the soil through stiffening.

Besides the levels of vibration attenuation of the various available mitigation measures, railway operators also have to incorporate the environmental, economic and befitting aspects of each measure before choosing one measure over another for a specific project. In this direction, a promising technology that could represent a key point for the rail industry is that of introducing the novel concept of metamaterial within the transmission path, because of its straightforward application in the soil and the range of sustainable materials that could be used as inclusions, which in turn could reduce the final production cost.

Metamaterials are artificial periodic elastic structures of scattering inclusions located in a structure or material [5,6], where the periodicity of these structures is represented by different unit cells with their periodic boundary condition replicated in the geometrical space, see Fig. 2. When engineering these crystals, it is possible to isolate vibrations within a certain frequency range, referred to as the bandgap, which is attenuated by the interference caused by the mechanism of the periodic system [7]. This concept was originally driven from the very small scale of the phononic metamaterial from electromagnetism, and has since been investigated in recent years by researchers and has also been implemented to attenuate the undesired mechanical vibrations arising from ground transportation, use of machinery in construction sites and low-amplitude earthquakes. These types of vibrations propagate through the soil in the form of seismic waves and have much a higher scale [8], hence the name seismic metamaterial.

In the civil engineering industry, there are different applications of seismic metamaterial, especially for building protection from the action of earthquakes [9,10]. Some recent research has also applied the expanded concept to the mitigation of vibrations generated by rail traffic, which has shown promising results. Yet, the available research is limited in terms of different ranges, such as the case of train configurations considering just the case of High-Speed trains and only using one type of material for the inclusions (generally concrete) [11–13]. The concept of artificial metamaterial has recently also extended to natural configuration [14], yet this is outside the scope of this research.

Although previous research [15] has shown higher costs and carbon emissions for the metamaterial with steel inclusions compared to other mitigation measures, such as open trenches, this is the case for only one type of inclusion, and open trenches require higher costs for maintenance, as presented by Ouakka et al. [4]. In another investigation [13], the concept of seismic metamaterial in the case of concrete inclusions has been briefly compared with other types of mitigation measures (such as dynamic vibrator absorbers and resilient wheels) and the metamaterial composed of concrete piles emerged to be the most suitable for the case of the LRV tram, the model presented in this study.

For this reason, this paper aims to increase the range of applications of metamaterial towards the vibrations generated by rail traffic, by extending their application to urban trams, which are the rail systems that cause the highest levels of vibrations in urban areas. In particular, the focus is on the T2000 tram running in Brussels on a ballast track. This is a representative vehicle for the investigation of the induced vibrations generated by rail traffic, due to its low floor design with a BA2000 bogie that is characterised by independent rotating wheels and motors mounted inside the wheels, causing the high level of generated vibrations when it goes over obstacles like crossings, turnouts, or rail joints.

The railway environment of the Brussels tram is reproduced using the numerical model already validated based on a two-step approach [16]. This approach is organised into two separate and successive steps. In the first step the vehicle/track subsystems are modelled with the in-house framework Easydyn to compute the forces applied by the track to the soil. In the second step, the outputs of the first step are applied to the soil implemented in the commercial finite element software ABAQUS. In particular, during the second step related to the soil modelling, a group of four-by-four piles is introduced in order to reproduce the metamaterial concept within the model. As previously mentioned, to implement the available application in the literature, an extensive parametric investigation was conducted for this study. This investigation studied four different types of material for the inclusion of the metamaterial in the soil: concrete, steel, wood and empty. Additionally, a span of the representative velocities for the T2000 tram was considered, starting from 10 [km/h] up to 80 [km/h].

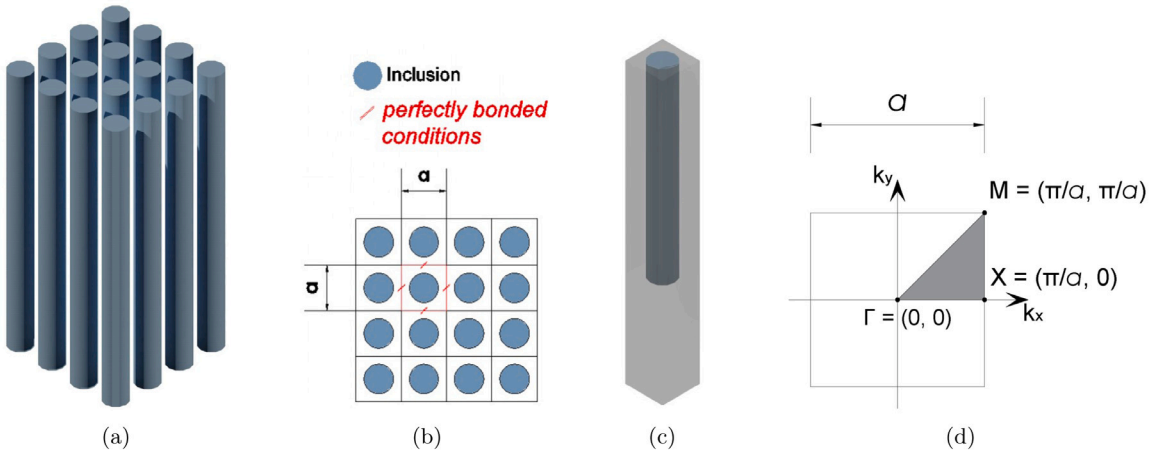

Fig. 2. Graphic representation of the seismic metamaterial: (a) 3D view of a periodic array of barriers, (b) metamaterial bird's eye view with Perfectly Matched Layers (PML), (c) 3D view of the unit cell and (d) first Brillouin zone with the irreducible part (light grey triangle of vertices Γ, X, M).

Further to this extensive parametric investigation, additional configurations of inserted metamaterial were evaluated in order to have a clear vision to what extent the number of rows of piles affects the attenuation, i.e. by considering groups of four-by-one, four-by-two and four-by-three piles. In this way is possible to have a direct relationship between the levels of the achieved attenuation and the material usage (and therefore the costs), allowing possible future applications to select the best configuration for any specific attenuation target.

Finally, the paper gives an evaluation of the global vibration attenuation levels at different distances and within the selected range of velocity, by presenting the attenuation levels in terms of the insertion loss [dB]. It also gives some insights into how this new technology of metamaterial can be set in order to make the most of it in the attenuation of railway vibrations in the case of urban areas and beyond.

2. Dispersion theory for periodic barriers

Seismic metamaterials could play a fundamental role in solving the problem of induced vibrations generated by railway traffic, thanks to their dispersion characteristics, which can help to enhance the attenuation levels of the existing mitigation measures.

In general, the attenuation of the induced vibrations can be quantified through wave dispersion theory inside the periodic metamaterials. Wave dispersion is illustrated in frequency domain, in which the different modes highlight the wave band gaps by considering the wavenumber k (along the vertices Γ - X - M) inside the unit cell (Fig. 2(d)), where the component k_x and k_y follow Eqs. (1) and (2) [17], taking into consideration a circular homogeneous inclusion with perfectly bonded materials, as highlighted in Fig. 2(b). The obtained band gaps represent the frequency region where the waves cannot go through the metamaterial and are therefore reflected. For this reason, it is important to understand how the seismic waves propagate in the metamaterial arrays and how these interact with the inclusions.

$$k_x = \begin{cases} (1-k)\pi/a, & \text{if } 0 < k < 1. \\ (k-1)\pi/a, & \text{if } 1 < k < 2. \\ \pi/a, & \text{if } 2 < k < 3. \end{cases} \tag{1}$$

$$k_y = \begin{cases} (1-k)\pi/a, & \text{if } 0 < k < 1. \\ 0, & \text{if } 1 < k < 2. \\ (k-2)\pi/a, & \text{if } 2 < k < 3. \end{cases} \tag{2}$$

where the value of $k = 0$, $k = 1$, $k = 2$ and $k = 3$ correspond respectively to the vertices M, Γ, X and M (in Fig. 2(d)) [17].

As previously mentioned, the band gaps give the range of frequencies for which the waves are reflected, this reflection could be considered for additional mitigation taking into account the damping of the material where these propagate. Yet, this is beyond the scope of this study.

2.1. Wave equation

The wave propagation equation for the incident plane waves in an isotropic linear material is described by the following Eq. (3) [18].

$$\frac{E}{2(1+\nu)(1-2\nu)}\nabla(\nabla u) + \frac{E}{2(1+\nu)}\nabla u = -\rho\omega^2 u \tag{3}$$

where u is the displacement vector and ω is the angular frequency. E, ν and ρ are Young's modulus, Poisson's ratio, and the density of the constituent materials, respectively.

2.2. Floquet–Bloch theory for periodic systems

In the case of periodic systems, such as seismic metamaterial, Eq. (3) can be solved for the periodic unit cell using the Floquet–Bloch theory [19]. Considering a periodic system with a square unit cell (i.e. $a = a_x = a_y$) with a period "a" and the periodic boundary conditions applied, the dispersion relations in Eq. (3) can be obtained according to the Floquet–Bloch theory as:

$$u(r + a) = u(r)e^{ika} \tag{4}$$

where a is the lattice vector, and $k = [k_x, k_y]$ the wave vector, as reported in Fig. 2(d).

2.3. Dispersion equation

From the combination of Eqs. (3) and (4), the dispersion equation in terms of eigenvalue is obtained, as in Eq. (5)

$$(\Omega(k) - \omega^2 M)u = 0 \tag{5}$$

where $\Omega(k)$ and M are the stiffness matrix and the mass matrix of the unit cell, respectively. The dispersion relation reported in Eq. (5) is a function of the wave vector k and the eigenfrequency ω. Therefore, in order to find the frequency modes, the wave vector should sweep along the path Γ, X, M, Γ (see Fig. 2(d)) in order to see its change across the boundary of the first irreducible Brillouin zone.

In this study to solve the eigenvalues equation the commercial software COMSOL was used, as will be presented later, and, by using some general assumptions available in literature [20], the band gaps were drawn in terms of dispersion curves.

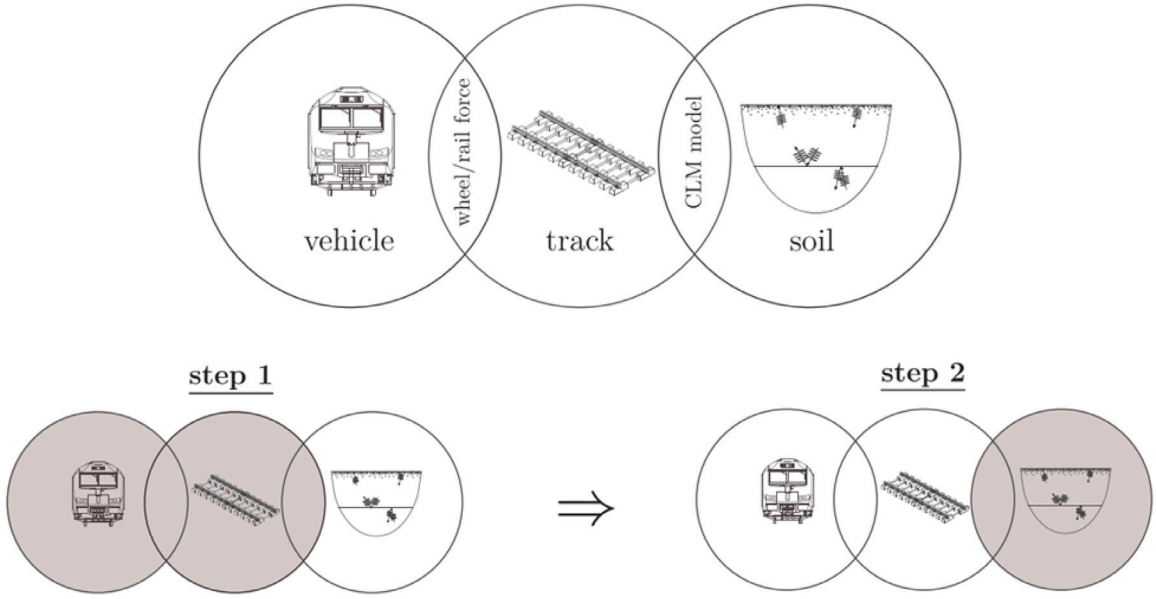

Fig. 3. Vehicle/track/soil model, decoupled between the ballast and the soil [21].

3. Numerical model of the railway environment

Different approaches are available to reproduce the railway environment to predict the induced vibrations in the soil caused by the train passage. In this paper, due to the aim of presenting a mitigation measure inserted within the transmission path, the two-step approach proposed [16,21] was used, see Fig. 3. The two-step approach consists of a first step that computes the dynamic behaviour of the vehicle/track subsystem using the multi-body software Easydyn [22], which uses the minimal coordinates approach to compute the forces applied by the vehicle/track subsystem to the soil. In the second step, the calculated loads were applied to the soil model implemented in the commercial Finite Element Software ABAQUS. Both simulations were performed in the time domain.

3.1. Vehicle/track subsystem

The T2000 tram, which runs on a ballast track, is used as a case study in this paper and is a representative vehicle in terms of the ground-borne vibrations generated by railway traffic due to its high level of vibrations [16]. The dynamics of the vehicle-track subsystems are simulated by considering a multi-body rigid vehicle model (Fig. 4(a)) with viscoelastic suspensions (Fig. 4(b)) moving at the speed V_0 on a flexible track (Fig. 4(c)) including a rail irregularity.

Values of the dynamic properties of the T2000 tram are reported in Fig. 4(b) with value in Table 1. The two external cars with the BA2000 bogie are composed of a mass car m_c, linked to bogie mass m_b with the moment of inertia I_b through a secondary suspension (k_2, d_2). In turn, the bogie mass is connected to the two wheel sets, one to the mass motor wheel m_m coupled to the bogie at a distance L_m by a primary suspension (k_m, d_m), and the other to a mass trailer wheel m_d linked to the bogie at a distance L_d by a primary suspension (k_d, d_d). With a total of six degrees of freedom. On the other hand, the central bogie is made of two motor wheels, such as the BA2000 motor wheel linked to the bogie at a distance L_b from the centre of the car.

The track (reported in Fig. 4(c) with respective values in Table 2) is defined as a flexible rail (Young's modulus E_r, a geometrical moment of inertia I_r, a section A_r and a density ρ_r), laying in the lumped mass m that plays the dynamic role of sleeper. The link between the rail-sleeper (rail pad) and sleeper-soil (ballast) is represented by a spring–damper system, respectively defined by its stiffness (k_p, k_b) and its damping (d_p, d_b). The wheel–rail forces are defined using non-linear Hertz's theory including the geometry of the potential defects, that allows the vertical coupling between the vehicle model and the track.

Table 1
Dynamic properties of the T2000 tram.

m_c	m_b	I_b	m_m	m_d
7580 [kg]	1800 [kg]	300 [kgm^2]	945 [kg]	160 [kg]
m_t	k_2	d_2	k_m	d_m
80 [kg]	960 [kN/m]	56.25 [kNs/m]	44 [MN/m]	18 [kNs/m]
k_d	d_d	L_d	L_m	L_b
5.876 [MN/m]	6 [kNs/m]	1.13 [m]	0.57 [m]	0.85 [m]

Table 2
Dynamic properties of the ballast track.

E_r	I_r	A_r	ρ_r	L
210 [GN/m^2]	1988 [cm^4]	0.00638 [m^2]	7850 [kg/m^2]	0.72 [m]
c_p	k_p	m	c_b	k_b
30 [kNs/m]	90 [MN/m]	90.84 [kg]	40 [kNs/m]	25.5 [MN/m]

3.2. Soil subsystem

The second step is characterised by the simulation of the soil subsystem with a finite element model. The soil is designed as a half-space composed of a central part made up of classical finite elements, surrounded by infinite elements, which help to reproduce the behaviour of an unbounded domain as depicted in Fig. 4(d). A 6-layered soil, with the characteristics presented in [23], and a uniform soil with the properties of layer 1 for a further investigation, see Table 3, are considered. For the present study, the induced vibrations transmitted from the train foundation are simulated using the finite-element software ABAQUS, which adopts the needed mapping formulation to link the central (finite) domain to the external (infinite) one [24], to avoid any reflection and to compensate any possible weakness of the mapping [25].

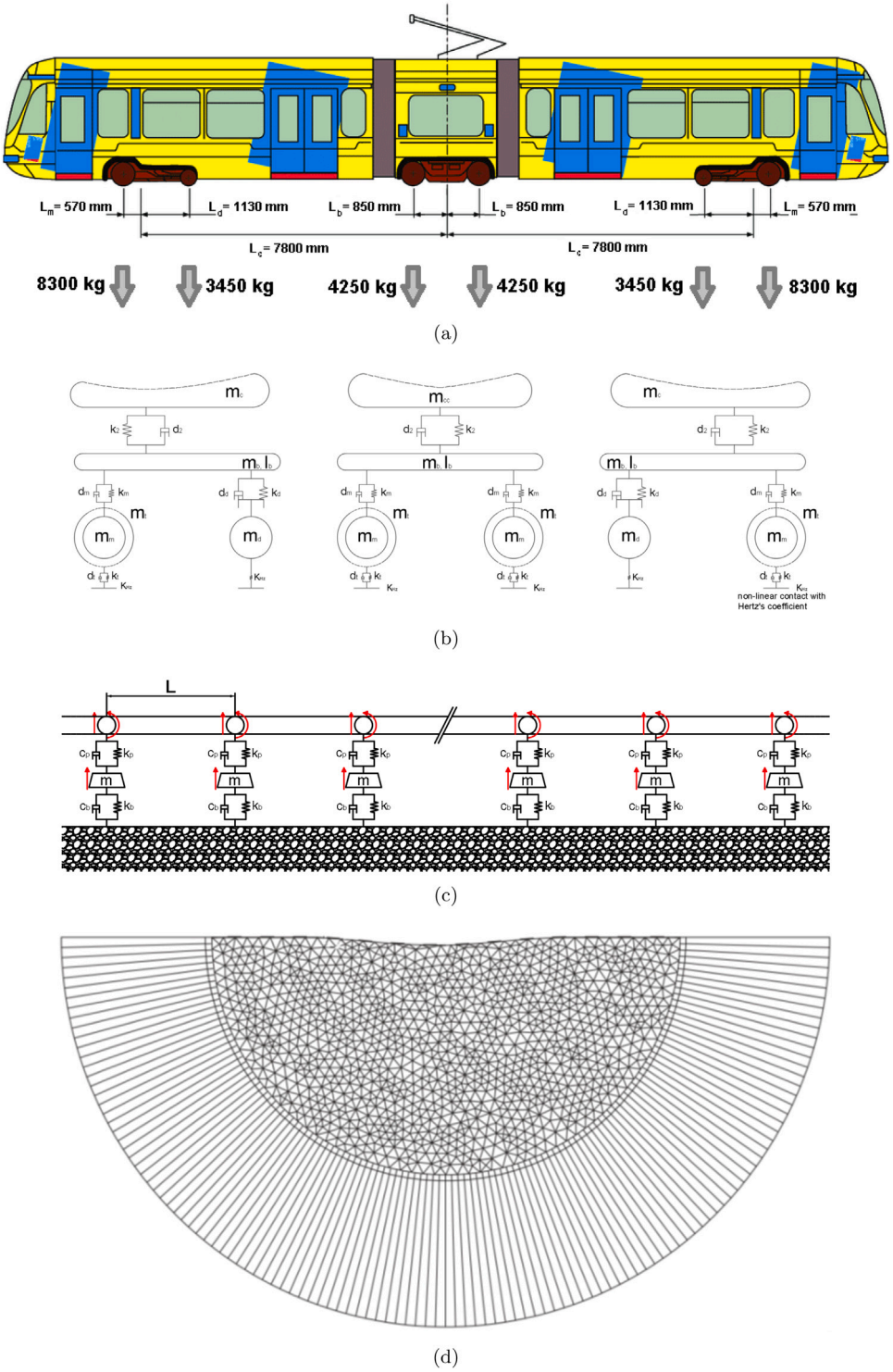

Fig. 4. T2000 Brussels tram details: (a) dimensions and axial loads, (b) rear, central "smaller" and front bogie, (c) track/foundation coupling and (d) half-sphere finite element model of the soil.

3.3. Seismic metamaterials

The considered seismic metamaterial mitigation measure can be seen as a group of piles inserted in an array disposition in order to reproduce the basic concept of the phononic material where the unit cell is repeated a range of times, as presented previously in this manuscript. In particular, a group of four-by-four pile arrays was considered within the second step of the utilised approach, i.e. by inserting it into the ABAQUS soil finite element model. The geometrical characteristics and material proprieties of the different configurations considered in the parametric investigation are summarised in Fig. 5, with the values reported in Table 4, with E, ρ and ν refereeing to Young's modulus, density and Poisson's ratio respectively. The geometrical dimensions of the three-dimensional unit cell are selected in accordance with [10,11].

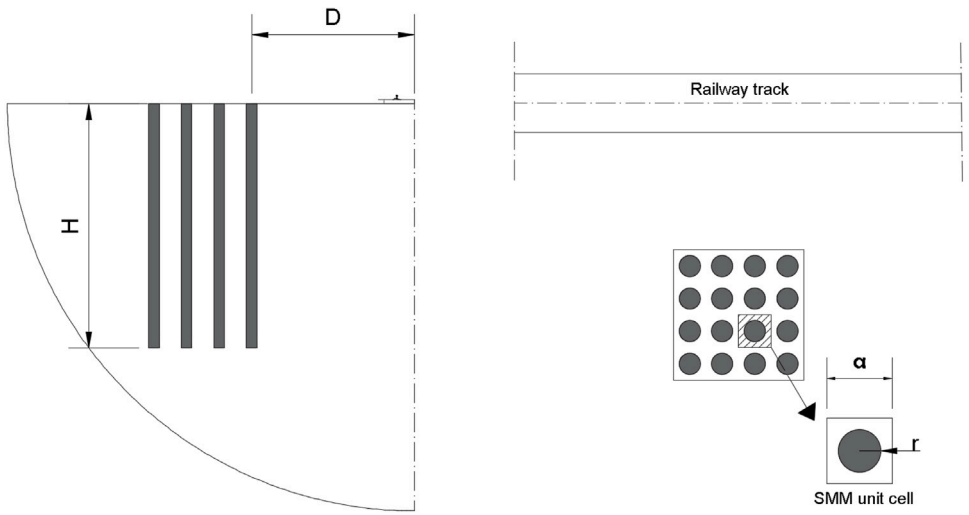

Fig. 5. Distribution of the piles array in the model, with details of the seismic metamaterial units.

Table 3
Soil proprieties and layering [23].

	E [MPa]	ρ [kg/m^3]	ν	h [m]	Viscous damping [ms]
Layer 1	61	1876	0.13	1.2	0.4
Layer 2	84	1876	0.13	1.8	0.4
Layer 3	287	1876	0.13	1.0	0.4
Layer 4	373	1876	0.27	1.0	0.4
Layer 5	450	1876	0.33	1.0	0.4
Half-space	465	1992	0.48	–	0.4

Table 4
Geometrical characteristics and material proprieties of the embedded seismic metamaterial.

Geometrical characteristics	D [m]	H [m]	a [m]	r[m]
	10	15	2	0.65
Material proprieties	E [MPa]	ρ [kg/m]	ν	Viscous damping [ms]
Concrete	40000	2500	0.2	0.4
Steel	210000	7850	0.3	0.4
Wood	1670	450	0.24	0.4
Empty	//	//	//	

To notice that the distance 'D' of 10 [m] from the centre of track is selected since is the most appropriate for the application of this measure, in order to prevent any opposite effect on the track that might be caused by the refraction of the waves exercised by the measure, likewise not to far to permit its applicability in urban areas.

4. Numerical validation of the models

Numerical models are certainly the appropriate solution to improve and conceptualise the new ideas of mitigation measures in the railway environment, as used in this research, to remain within feasible costs. Yet to achieve reliable results for the final field implementations, numerical models have to be validated against field measurements or other numerical results. In particular, in this section, the different validations for the numerical tool used in the paper will be presented. Starting from the validation of the vehicle/track/soil model against field results, then the validation of these results after the introduction of the geometry of the inserted piles in order to check that this does not alter the wave propagation within the soil. Finally, the metamaterial is validated with a previous numerical model to predict the level of attenuation for the selected geometrical and material proprieties.

4.1. Previous validation of the T2000 model

Field measurements have been conducted to validate the complete model in terms of the generation and propagation of the vibrations within different representative situations [16,26]. In particular, here the validation of the reference case without any mitigation measure is taken into consideration, by comparing the vibration time history of the numerical reference case of the T2000 tram and the in-situ measurements.

Fig. 6 presents the vertical velocity of the ground of the used model compared with the in-situ measurements conducted at the Haren site, in the Brussels Region [27,28], considering a tram velocity of 30 [km/h], with a local defect. In particular, Fig. 6(a) presents the vertical velocity 2 [m] from the track, while Fig. 6(b) shows it 8 [m] from the centre of the track. Although at both distances the numerical peaks are slightly lower than the field ones, the velocity time history is well captured showing a reasonable agreement between the numerical model used in this study and the field data. Additionally, the frequency domain validation for the in-situ results in the case of a single car bogie was presented by Kouroussis et al. [28].

4.2. Inclusion of metamaterial in the FE soil

Before moving to the vibration history results for the different metamaterials, it is crucial to have a validation of the model as it is very sensitive to meshing. The mesh map of the soil model is changed because of the introduction of the inclusion in the geometry, which considers the edges of the group of piles. The validation of the new mesh map (where the inclusion is considered) is shown in Fig. 7 where the time history acceleration has a good agreement with the original mesh (without inclusion).

4.3. Transmission of the phononic material

In addition to the mesh validation of the inserted seismic metamaterial illustrated in the previous Subsection, it is important to have a prior evaluation of the level of attenuation of the specific metamaterial before introducing it into the finite element soil developed in ABAQUS. The evaluation of the attenuation of the investigated seismic metamaterial is identified through the drawing of the dispersion curves obtained in turn by solving the wave equation presented in Section 2.1.

In order to do this, two models of the unit cell were built using the commercial finite element software COMSOL, which allows the wave dispersion equation to be solved and the dispersion curves

Table 5
Reference material proprieties and geometric characteristics.

Metamaterial	Density [kg/m^3]	Young's Modulus [MPa]	Poisson's ratio	a [m]	r [m]	H [m]
Concrete [8]	2500	40000	0.20	3	1.20	6
Soil	1800	20	0.30			
Steel [10]	7850	200000	0.33	2	0.60	15 + 0.8 (in bedrock)
Soil	1800	153	0.30			15
Bedrock	2500	30000	0.30			5

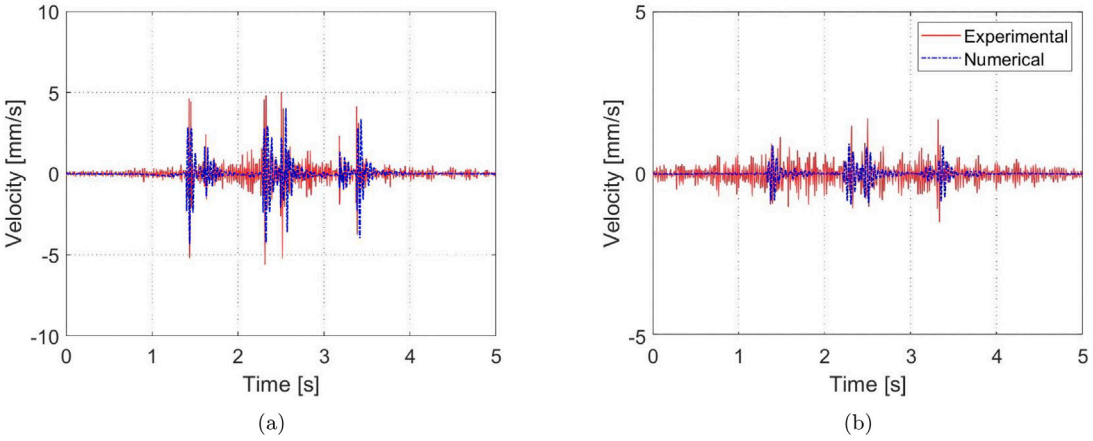

Fig. 6. Vertical ground velocity during the passing of the T2000 tram at speed v_0 = 30 [km/h] on a rough rail with a local defect: (a) 2 [m] from the track and (b) 8 [m] from the track.

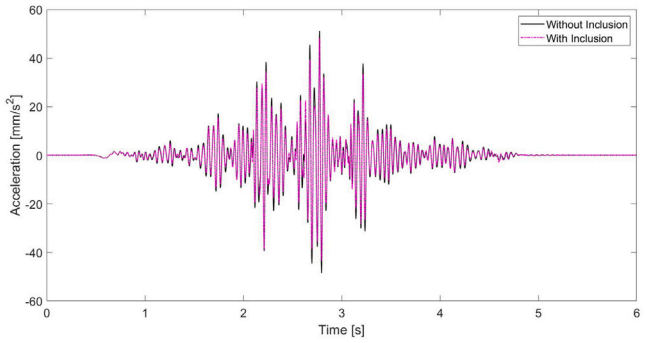

Fig. 7. Mesh validation after the introduction of the inclusion, vertical acceleration at 18 [m] with a tram speed of 60 [km/h].

to be drawn. This then is validated against the results presented in previous research [8,10], with the material proprieties summarised in Table 5, with the nomenclature in accordance with Fig. 5. The same assumptions as in the references were considered i.e. perfectly matched layers (PMLs) are applied at the two edges of the soil parts to prevent reflections by scattering waves from the domain boundaries.

In particular, for the first Ref. [8] with concrete inclusion the top and bottom faces are considered simply as free edges in order to allow their free movement, resulting in Fig. 8 showing the perfect match. Where the band-gap (between 26.5 [Hz] and 29 [Hz]) is a consequence of the two eigenmodes, A and B, which are below and above the identified band-gap. On the other hand, for the second Ref. [10] with steel inclusion, a rigid bottom part is included where the pillar is embedded with a length of 0.8 [m] to create a bandgap starting from zero with the first enginemode (C) at 4.6 [Hz], as depicted in Fig. 9, where the dispersion curves are reported. In the developed model, some displacements can be seen from the reference case close to the Γ the centre of the unit cell, these are negligible.

Before moving to the analysis of the attenuation levels within the soil propagation, it is worth moving forward from the references by considering a realistic case where the model is no longer clamped, as presented the in literature [10]. A third numerical model composed of a line of four pillars was built in COMSOL (as shown in Fig. 10(a)) by considering a stiffer layer below the substrate to prevent any reflection of the bottom waves to the surface, with an unclamped pile [10]. In particular, the developed model consists of one row of piles in the x direction. In the y direction, the phononic crystal (PnC) was assumed to be periodic, therefore periodic boundary conditions are used in this direction. Given that the soil is semi-infinite in the z direction and infinite in both the x and y directions, in the simulation, the soil was considered to be of finite size and, to avoid the reflection of elastic waves at the boundaries of the soil, the PML condition was used at the bottom as well as on both sides of the soil. The excitation of the surface acoustic waves at the entrance of the PnC was performed by applying a force in the vertical direction of the soil surface and the detection was done at the detector of the PnC (position in Fig. 10(a)). To solve the associated wave equation, triangular was applied for the piles and the soil domains and a mapped mesh was applied for the PML domains. The maximum element size was fixed to 0.5 [m] at the surface of the soil and was increased to 2 [m] towards the bulk of the soil, and the complete mesh consisted of 229,970 elements. At the same time, the same geometrical characteristics and material proprieties in Table 4 were used in order to be able to later compare the attenuation levels with the full analysis obtained using the two-step approach that will be presented later in this manuscript, in Section 5. The final model was validated against the results of [29].

In Figs. 10(b) and 10(c) the surface wave transmission curves for the ΓX and ΓM direction respectively (calculated according to Eq. (6)) are plotted against the frequency in the range from 0 to 50 [Hz]. In the ΓX direction the highest drop in the propagation can be seen above 20 [Hz] for three of the inclusions (concrete, steel and empty) with empty presenting a significant peak around 46 [Hz], as depicted in Fig. 10(b). Whereas, in the ΓM direction in Fig. 10(c) the drop for the steel inclusions is above 27 [Hz] and after 44 [Hz] for the concrete. In the same plot the raise of the transmission for the wood with respect to the empty inclusions can be noted. For the empty inclusion, the transverse branch is folded at low frequency (at 20 Hz in ΓX direction) contrary to that of the wooden inclusion.

$$Transmission = \frac{u^{p.c.}}{u^{subst.}} \tag{6}$$

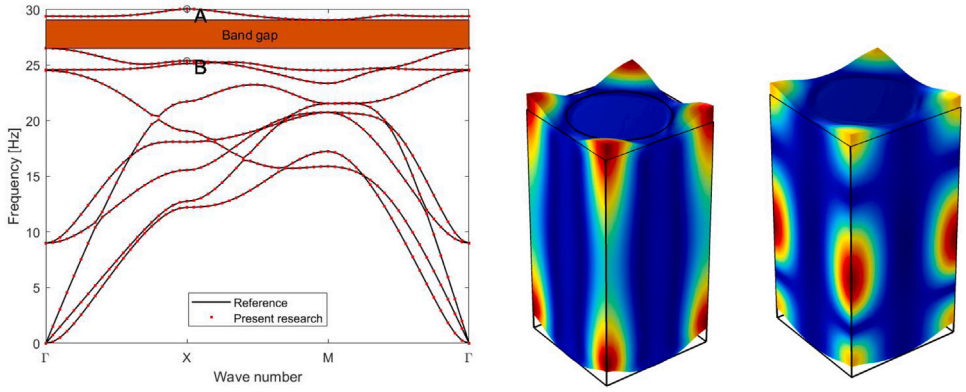

(a) Dispersion curves with band gaps (b) Eigenmode in point A (c) Eigenmode in point B

Fig. 8. Concrete model validation compared with the reference case [8].

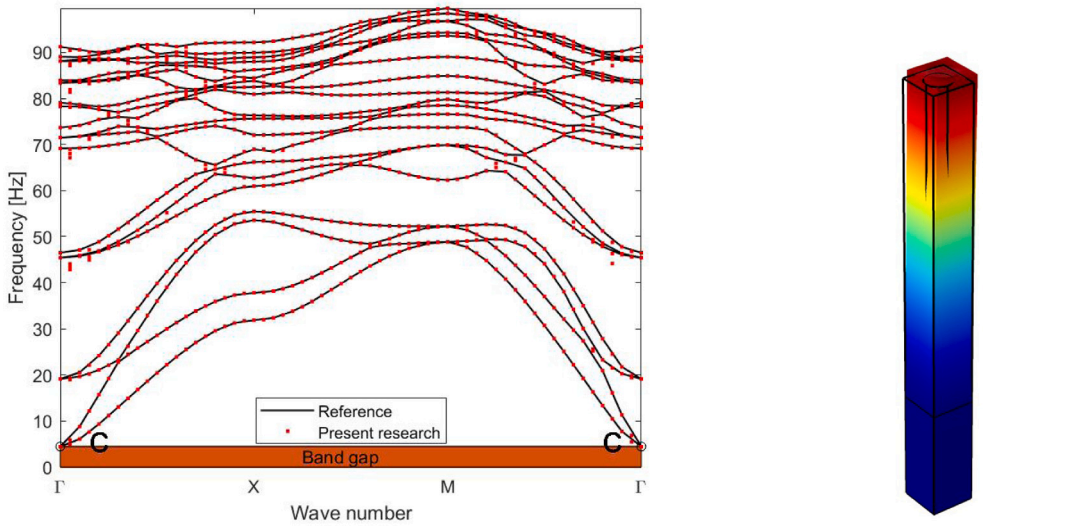

(a) Dispersion curves with band gaps (b) Eigenmode in point C

Fig. 9. Steel model validation compared with the reference case [10].

where $u^{p.c.}$ is the propagated velocity when the phononic crystal is considered and $u^{subst.}$ is the velocity without the mitigation measure where the wave propagation in the substrate (in our case the soil) is taken into account.

5. Vibration time history results and discussion

In this section, the vibration time history of the model with the seismic metamaterial introduced is compared with the case without any mitigation measures in order to evaluate the possible advantages in terms of the vibration reduction obtained by using this new technology.

5.1. Reference case

The reference setup considered to compare the different characteristics has a lateral distance of 18 [m] from the centre of the track (in order to take into consideration the effects after the group of piles) and a tram speed of 60 [km/h] (which is the most representative speed). The vibration time history analysis is shown in Fig. 11 for the different inclusions: concrete (Fig. 11(a)), steel (Fig. 11(b)), wood (Fig. 11(c)) and empty (Fig. 11(d)), with the proprieties of each inclusion reported in Table 4. A good level of attenuation was obtained for all the filled inclusions, reaching a reduction of the peak velocities of 55%, 46% and 54% for the concrete, steel and wood respectively. This also meets the prediction for the case of empty inclusion where the smallest reduction was seen.

Furthermore, from the evaluation of the distribution of velocity amplitudes depicted in Fig. 10, a good reduction in terms of amplitude velocity can be noted, where the most attenuated frequencies were the ones above 10 [Hz] for all four of the inclusions, with a very strong minimisation in the range of 20 to 30 [Hz] for the case of inclusions. The noticeable reduction from the latter vibration velocity time history is explained by the refraction that the metamaterial exerts against the wave propagation. It can be seen well from the velocity propagation in the finite element soil model developed in ABAQUS. In particular, for the reference case, the maximum velocity was reached around the time 2.7 [s] (as can be seen in Fig. 11) approximately when the centre of the tram was at around 28 [m] from the left edge of the 50 [m] model. By comparing the FE plan view at this instant (2.7 [s]) of the case without inclusions in Fig. 12(a) and the four cases of different metamaterial inclusions in Figs. 12(b)–12(e), there is a further confirmation that for the case of concrete and steel inclusions, in Figs. 12(b) and 12(c) respectively, there is strong refraction of the waves exercised by the metamaterial. A smaller deflection of the waves can be seen for the case of wood inclusions, in Fig. 12(d), yet this is not the case of empty inclusions where no evident alteration in propagation is seen, as reported in Fig. 12(e).

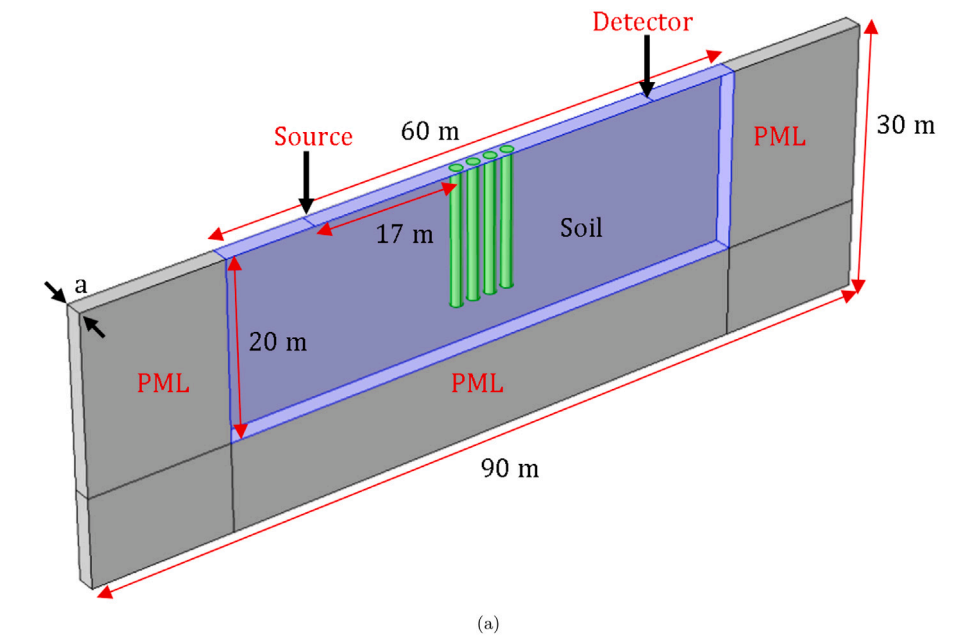

(a)

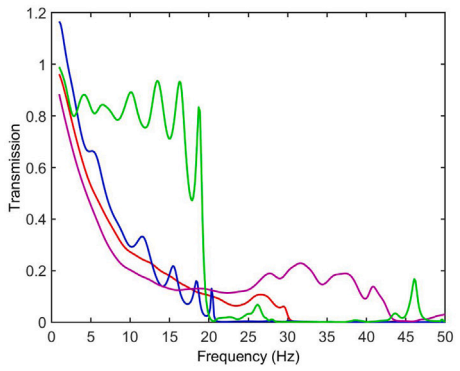

(b)

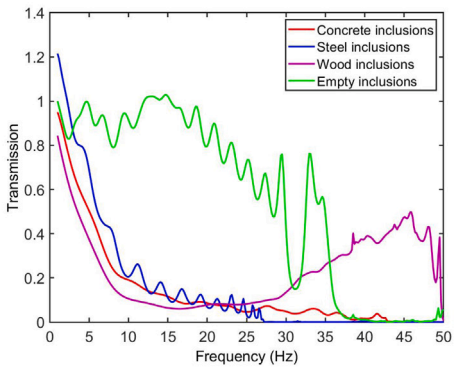

(c)

Fig. 10. Developed pile array model in COMSOL: (a) COMSOL 3D model dimensions, (b) transmission ΓX direction and (c) transmission ΓM direction.

Although the performed simulation is in the time domain, by applying a Fourier Transformation of the vibration velocity, for the representative speed of 60 [km/h], it is possible to see how the amplitudes are affected by the introduction of the investigated mitigation measures, as depicted in Figs. 13 and 14 for the lateral distances of 8 [m] (just before the metamaterial) and 18 [m] (just after the group of piles). From these results, it is straightforward to notice, as expected, an increase in the amplitudes just before the metamaterial due to the refraction of the waves exerted by the group of piles (Fig. 13) especially at high frequencies, i.e. above 30 [Hz], with an increase of the maximum amplitude in the case of empty inclusion. Conversely, in the case after the group of piles (Fig. 14), a decrease of the amplitude is notable with a strong reduction of the maximum amplitudes for all the filled inclusions.

Some shifts between the FE model in Fig. 14 and the case of transmission obtained with COMSOL reported in Fig. 10 arise from the fact of the consideration of an ideal infinite metamaterial in COMSOL that does not precisely reflect the superposition of the effects that can arise from the four-by-four pile modelled in ABAQUS. Yet, the predicted trend is preserved for each of the four inclusions, where the concrete and the steel inclusions show the best attenuation with the predominance of the steel around 20 to 30 [Hz]. Therefore, the use of COMSOL analysis is justified as a preliminary parametric investigation that can help in setting the best geometrical and material proprieties for a given range of frequencies.

5.2. Comprehensive parametric investigation

To consider the additional parameters that could affect the attenuation levels, a further parametric investigation was conducted, by considering a range of material proprieties for the inclusions, as well as considering a range of velocities from 10 [km/h] to 80 [km/h], which represents the characteristics of the T2000. It is worth introducing the standard evaluation in terms of insertion loss (IL) which gives a standard evaluation of the attenuation in [dB], and is obtained as the difference in vibrations, between the original configuration and the application of the measure. In other words, the IL is obtained as shown in Eq. (7) from the ratio of the particle displacement of the configuration without and with the mitigation measure [4]:

$$IL = 20\log_{10}\frac{u^{ref}}{u} \tag{7}$$

By considering the different distances (range from 2 [m] to 20 [m]), it is also possible to investigate how the group of piles affects the time history of the propagation of vibration waves, as depicted in terms of IL, for all four types of inclusion. From Fig. 15 it is straightforward to understand the negative insertion loss at 8 [m] is caused by the refraction of the metamaterial that leads to a higher velocity. However, the positive effects can already be seen inside the group where an IL of 10 [dB] is reached (case of steel inclusion).

Furthermore, by taking into consideration different distances (from 2 [m] to 20 [m]) and a range of velocities (from 10 [km/h] to 80

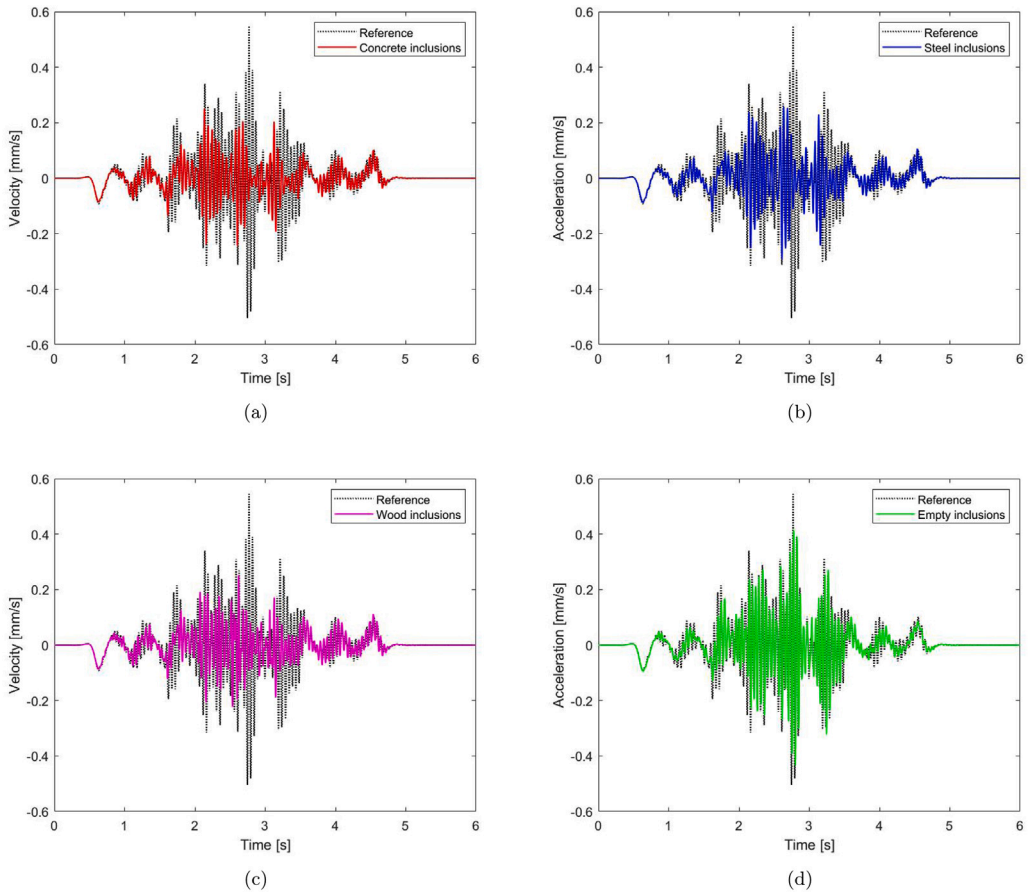

Fig. 11. Vibration time history analysis in the case of metamaterial 18 [m] from the centre of the track with a tram speed of 60 [km/h]: (a) concrete inclusions, (b) steel inclusions, (c) wood inclusion and (d) empty inclusion.

[km/h]), it is possible to have the whole picture of the effect of the metamaterial, as reported in Fig. 16. In the case of the unique speed of 60 [km/h], there is the presence of a negative IL just before the group of piles and a positive IL already from inside the array for all three filled with inclusions (concrete, steel and wood). Whereas, in the case of empty inclusion the negative IL was also noticeable inside the array because no material is there to produce the scattering effect, as also emerged in the velocity time history analysed previously.

5.3. Additional parametric investigation

In addition to the results illustrated previously for the comprehensive parametric investigation, it is worth extending the range of the latter to better evaluate the obtained results and assess them to drive the physical behaviour of this technique. In particular, the first extension will be on the soil characteristics going from a layered soil to a uniform one, followed by a second enlargement in which different row layouts of the metamaterial are considered.

5.3.1. Different soil characteristics

The role of the hosting material (i.e. soil in the present study) of the inclusion is very important in understanding the feasibility of metamaterial in the railway industry. Indeed, the underground soil characteristics change randomly through the length of the rail grid. Even though this variation can be revealed with an in-situ geotechnical test it is usually limited to specific points of the surrounding areas due to the high cost entailed, which is not justifiable for the whole area.

Therefore, to understand how the shifting of the soil characteristic can affect the level of attenuation, the same parametric investigation was repeated for the case of steel inclusions (being the one showing the best levels of attenuation) by considering a uniform soil with the first layer characteristic of the previous investigation (as reported in Table 3 [23]) for the complete soil model.

Firstly, by comparing how the propagation of wave changes from the more realistic layered case to the uniform one (without the mitigation measure), a comparison in terms of IL was done, as depicted in Fig. 17. From the figure, it can be noticed that the uniform case has a relevant increase in the IL because the deeper layer, in the case of layered soil, is stiffer and drives the vibration waves to propagate on the surface rather than in the bulk.

Therefore, as also expected in the case of the mitigation the IL is higher for the uniform soil, as reported in Fig. 18. Yet, the trend of the IL can be seen following the same uniform path, if the distance of 20 [m] is considered, and this decreases with the increase in the velocity.

5.3.2. Supplementary metamaterial layouts

For this case of considering different rows of metamaterial the reiterated representative velocity of 60 [km/h] is examined, as well as the case of inclusions made of steel, to evaluate the magnitude of changes when the number of rows changes. As such, the primary four-by-four metamaterial will be compared with the case of one, two and three rows of four piles with the distance of the first row of each always kept at 10 [m]. These layouts are reported in Fig. 19. The consideration of fewer rows is interesting, not only in terms of costs but also in terms of space usage since the reduction of a row for the present case means 2 [m] less where it is possible to find existing buildings or to be able to build others, especially for urban areas.

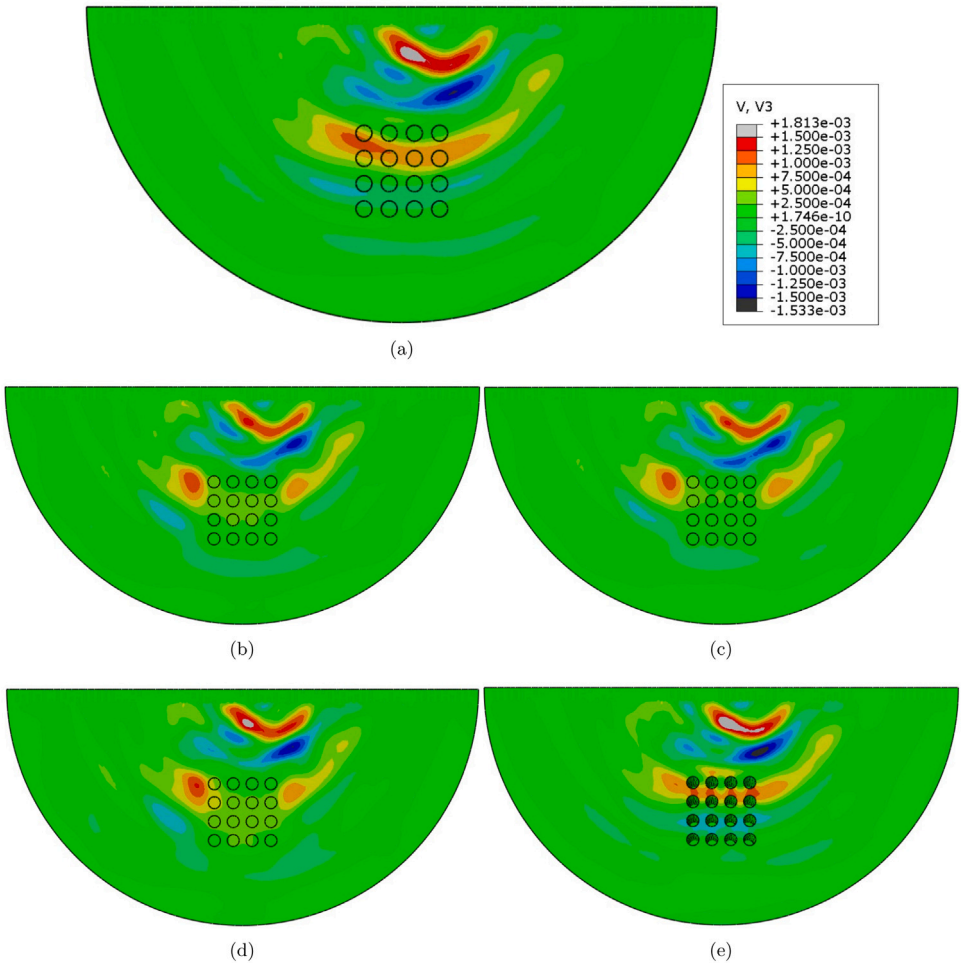

Fig. 12. Plan view of the outlines of the velocity wave propagation at time 2.7 [sec] (centre of the T2000 28 [m] from the left corner): (a) reference case, (b) concrete inclusion, (c) steel inclusions, (d) wood inclusion and (e) empty inclusions.

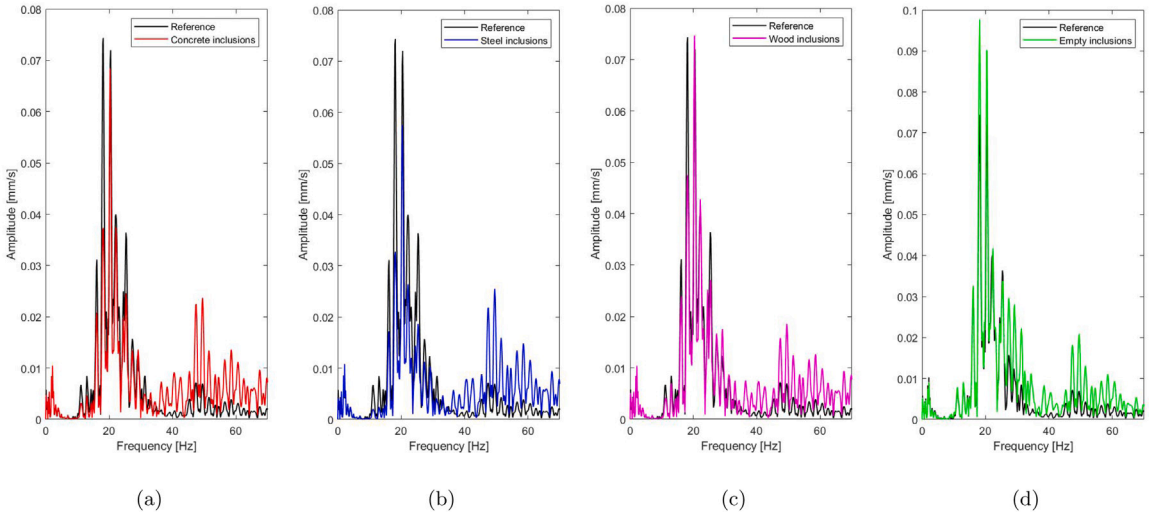

Fig. 13. Frequency distribution at a lateral distance of 8 [m]: (a) concrete inclusions, (b) steel inclusions, (c) wood inclusions and (d) empty inclusions.

Fig. 20 shows the different IL at the different lateral distances for the three new configurations. In particular Figs. 20(a) and 20(b) consider, as a reference, the model without any measures and the model with the inclusion of the four-by-four group of piles respectively. These show important alterations before, inside and after the metamaterial inclusions. At the beginning of the group of piles (at a lateral distance of 8 [m]) the vibration attenuation in terms of IL is inversely proportional to the row of the piles, in other words, the attenuation increases when the number of rows decreases, as reported in Fig. 20(b), and this can be due to the lower strength of all the blocks of piles. Whereas inside the group of piles (from 10 to 18 [m]) the attenuation does not follow a general trend, due to the difference in the ending of each layout that

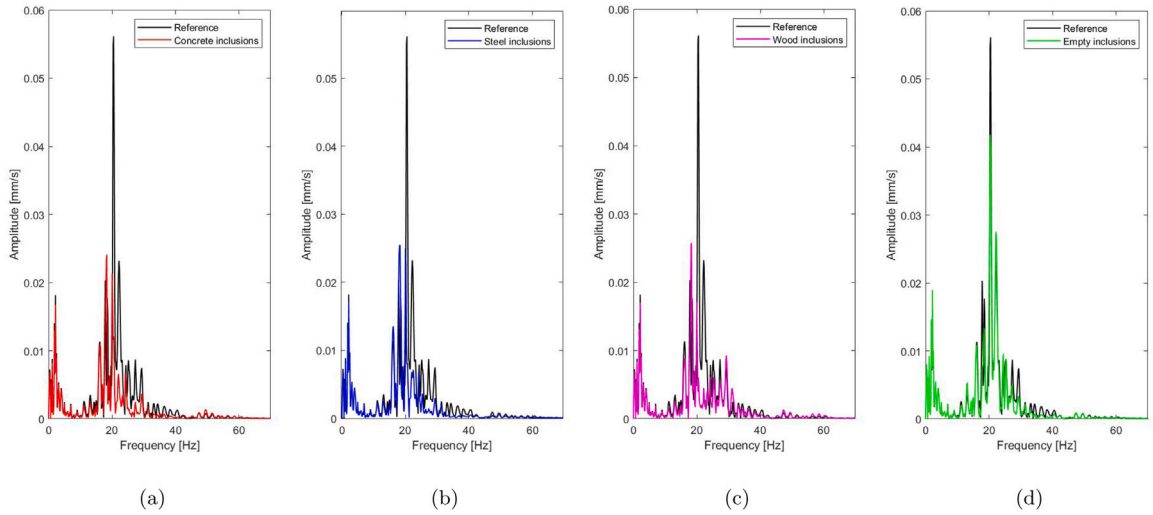

Fig. 14. Frequency distribution at a lateral distance of 18 [m]: (a) concrete inclusions, (b) steel inclusions, (c) wood inclusions and (d) empty inclusions.

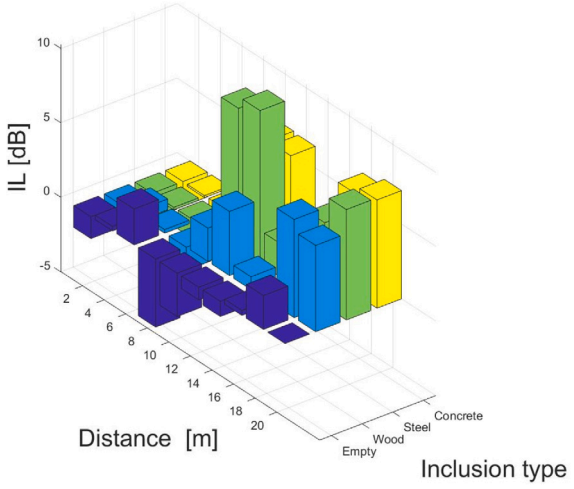

Fig. 15. Insertion loss at different distances for the embedded metamaterial, speed of 60 [km/h].

affects the interaction of the wave propagation. For example, the lateral distance of 14 [m] is behind the configurations of one and two rows of piles but still inside the case of three and four rows.

Furthermore, if a distance of 20 [m] behind the four-by-four is considered, this allows the final effects of all the layouts to be considered. It can be noticed that for the case of one and two rows, as expected, there is a decrease in the IL, whereas, the three-by-four shows a high IL, as represented in the bar graphs in Fig. 21. This odd enhancement of the three rows layout is due to the interaction that the waves have with the two arrays inside the lattice structure and the particular frequency that this is able to manipulate.

6. Conclusions

Induced vibrations generated by rail traffic is an important subject of concern among the residents of urban areas, and the main drawback which might slow down the development of the railway system as a principal means of transport. Indeed, this could be problematic for the goal to reduce global carbon emission. For this reason, over the past few years, different researchers have focused their attention on possible mitigation measures to attenuate these effects. In spite of this fact, few of these measures can be found in actual projects in the railway industry, as they are often not attractive to investors due to their costs of construction and/or maintenance and the difficulty of application. Therefore, the development of a new concept that could overcome these limitations could be the right direction for the attenuation of the induced vibrations.

Seismic metamaterial represents an example of a possible new concept for which the application is well known in civil engineering, and has relatively low costs of application and maintenance. In this study, the possible levels of attenuation which can be reached have been investigated through a comprehensive parametric investigation by introducing them in a validated numerical model based on the two-step approach of the T2000 tram running in Brussels. Various parameters have been considered in the analysis. Four types of material for the inclusions have been considered, as have a range of representative velocities ranging from 10 [km/h] to 80 [km/h]. In addition, these were implemented by taking into account different layouts of the groups of piles and different materials for the transmission path. From the exhaustive parametric investigation the different aspects that emerged can be summarised as follows:

- The different levels of attenuation obtained by using the seismic metamaterial in the transmission path, after the array of the group of piles, justify its implementation and further research on the concept of metamaterials in the railway industry. These attenuations have shown an agreement, for the frequency affected, with the preliminary investigation based on the dispersion theory for periodic barriers simulated with COMSOL.
- The type of material used for the inclusions has a direct relationship, in terms of insertion loss, with the attenuation of the peak velocity, independently from the value of the velocity of the train. The order of reductions showed that the inclusions made of concrete and steel have the highest levels, followed by the inclusions made of wood. On the contrary, the empty one has, as expected, a negative value.
- The material of the hosting transmission path has a relevant importance in the propagation of the waves, including before reaching the metamaterial array, yet the insertion loss obtained after the inclusion had the same influence on the surface wave reaching that point, which is obviously not with the same amplitude due to the difference in the media of propagation.
- The different layouts considered in the extension of the parametric investigation conducted showed a direct improvement as a consequence of introducing additional rows to the metamaterial block. However, the configuration of three rows has a higher IL with respect to the original block of four rows, presumably caused by the response of the whole block to the propagation of the induced waves.

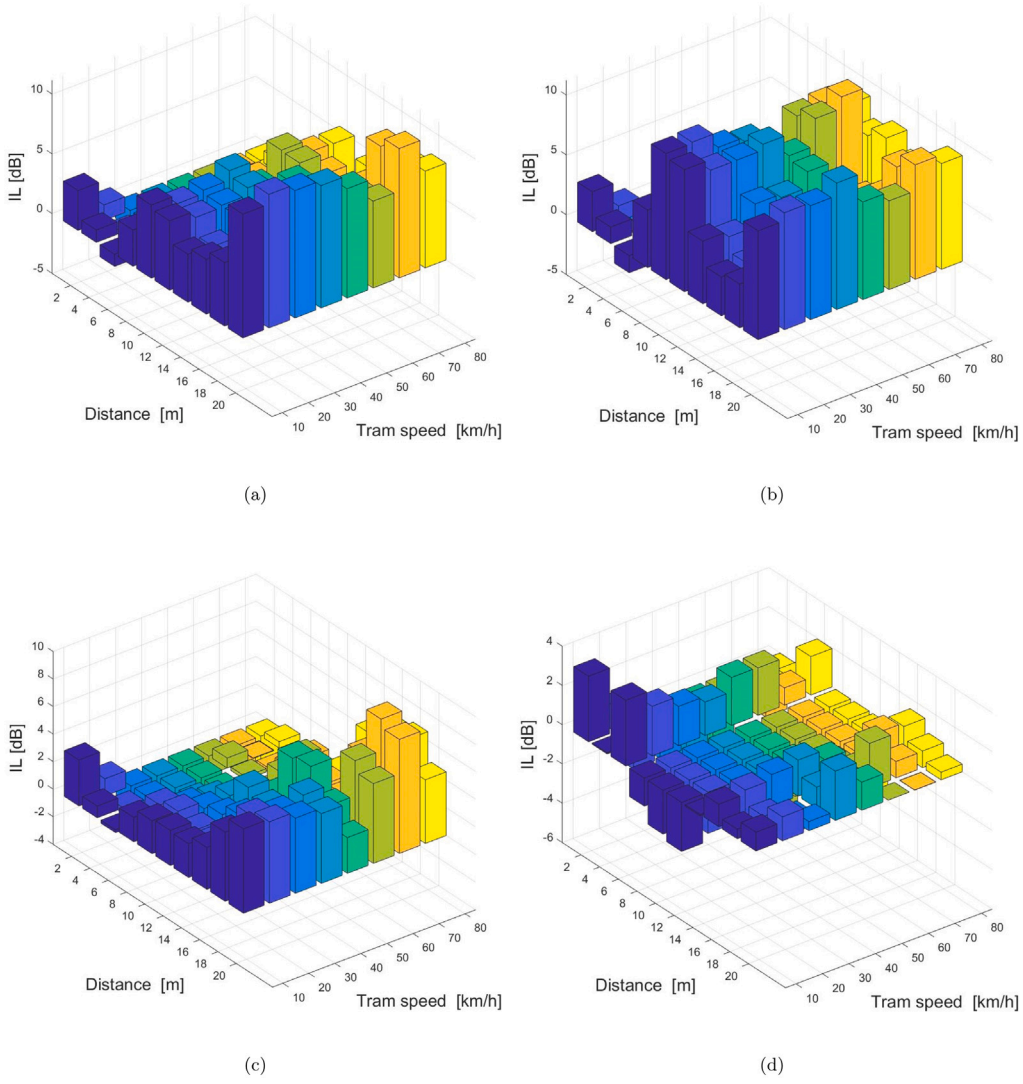

Fig. 16. Insertion loss parametric investigation: (a) concrete inclusions, (b) steel inclusions, (c) wood inclusions and (d) empty inclusions.

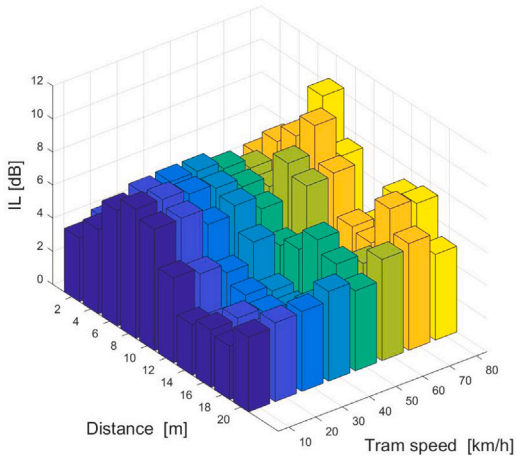

Fig. 17. Insertion loss from the layered to the uniform soil without inclusion.

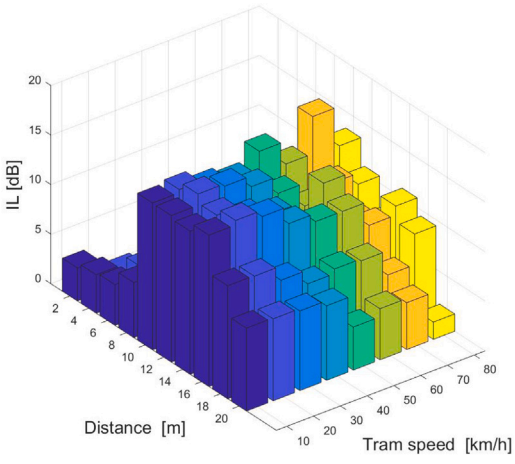

Fig. 18. Insertion loss from the layered to the uniform soil with steel inclusion.

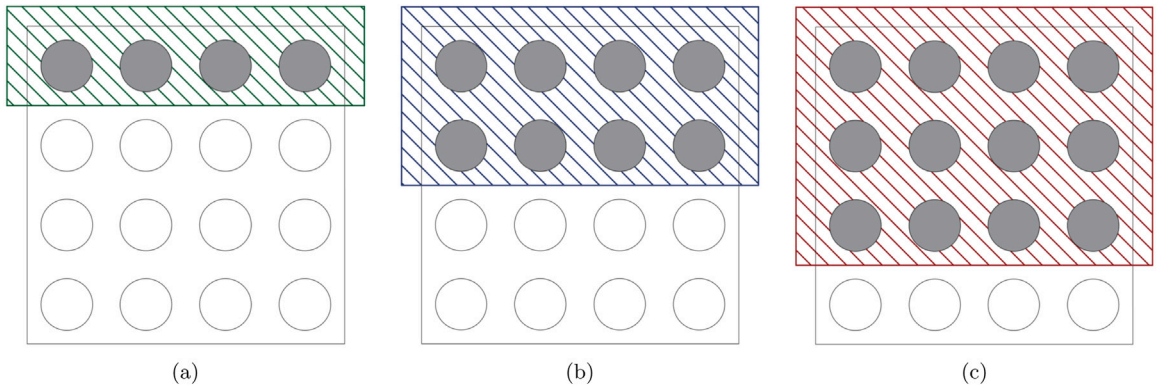

Fig. 19. Different metamaterial layouts: (a) one-by-four, (b) two-by-four and (c) three-by-four.

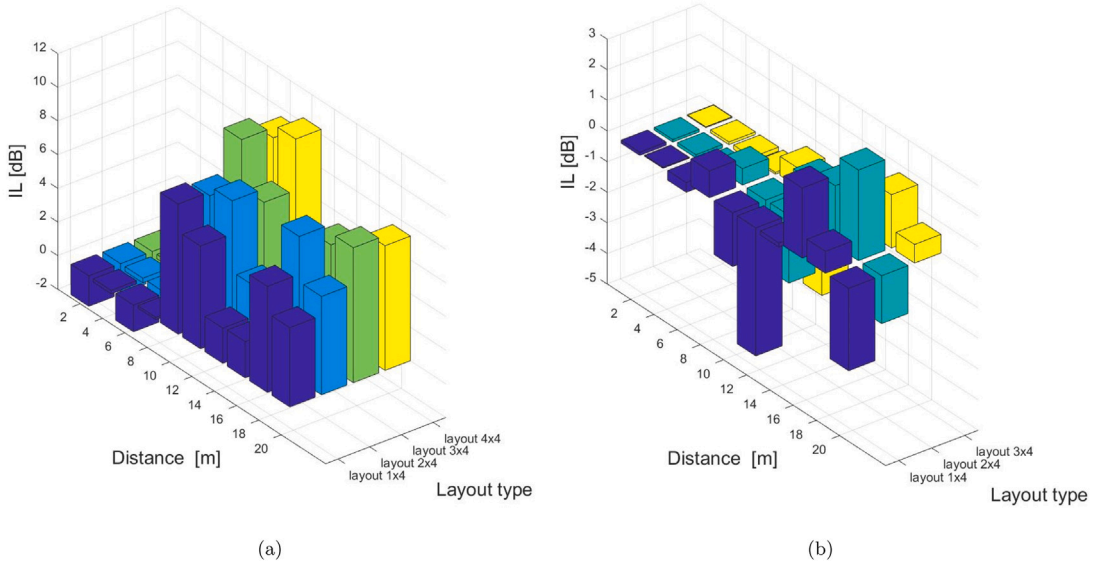

Fig. 20. Insertion loss for the different layouts, lateral distance from 2 to 20 [m] and tram speed of 60 [km/h]: (a) with respect to the reference model and (b) with respect to the 4 × 4 layout.

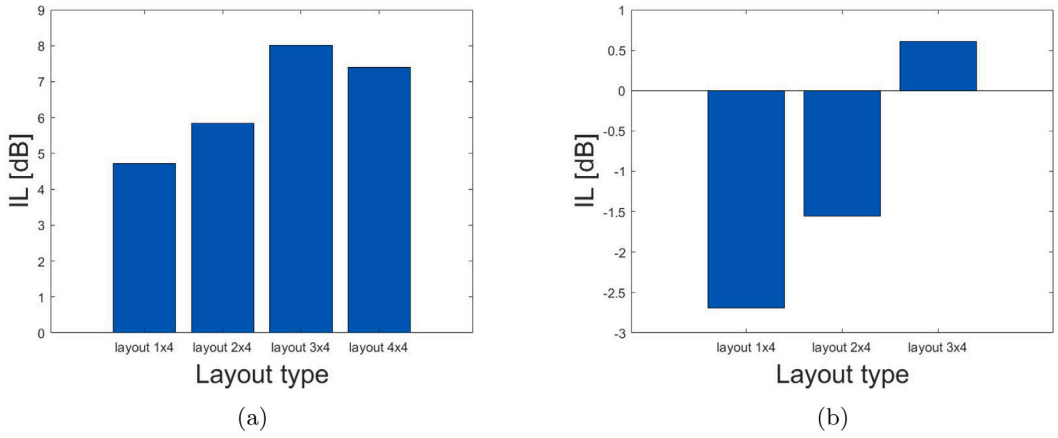

Fig. 21. Insertion loss for the different layouts, lateral distance of 20 [m] and tram speed of 60 [km/h]: (a) with respect to the reference model and (b) with respect to the 4 × 4 layout.

This study represents one of the first investigations of the novel concept of seismic metamaterials applied to the railway environment. With the positive outputs described in this manuscript, it can be concluded that the new concept of seismic metamaterials has great potential for the mitigation of induced railway vibrations. Certainly, this needs to be refined and implemented to cover a wider range of applications depending on the different train technologies available in the industry.

CRediT authorship contribution statement

Slimane Ouakka: Conceptualization, Methodology, Software, Writing – original draft, Validation, Visualization. **Abdellatif Gueddida:** Methodology, Software, Validation. **Yan Pennec:** Methodology, Writing – review & editing, Supervision. **Bahram Djafari-Rouhani:** Writing – review & editing, Supervision. **Georges Kouroussis:** Resources, Writing – review & editing, Supervision, Funding acquisition. **Olivier Verlinden:** Supervision.

Declaration of competing interest

The authors declare that they have no known competing financial interests or personal relationships that could have appeared to influence the work reported in this paper.

Data availability

Data will be made available on request.

Acknowledgements

This work was financially supported by the European Union's Horizon 2020 research and innovation programme under the Marie Skłodowska-Curie grant agreement No INSPIRE-813424.

References

[1] Kouroussis G, Kinet D, Moeyaert V, Dupuy J, Caucheteur C. Railway structure monitoring solutions using fibre Bragg grating sensors. Int J Rail Transp 2016;4(3):134–49.
[2] Ouakka S, Verlinden O, Kouroussis G. Mitigation measures dedicated to railway-induced ground vibration: An analysis of recent advances. In: 27th international congress on sound and vibration. 2021, (virtual conference).
[3] Hunt HEM, Hussein M. Ground-Borne vibration transmission from road and rail systems: Prediction and control. In: Handbook of noise and vibration control. John Wiley & Sons, Inc.; 2008, p. 1458–69.
[4] Ouakka S, Verlinden O, Kouroussis G. Railway ground vibration and mitigation measures: Benchmarking of best practices. Railw Eng Sci 2022;30(1):1–22.
[5] Sigalas MM, Economou EN. Elastic and acoustic wave band structure. J Sound Vib 1992;158(2):377–82.
[6] Deymier PA. Introduction to phononic crystals and acoustic metamaterials. In: Acoustic metamaterials and phononic crystals. Berlin, Heidelberg: Springer Berlin Heidelberg; 2013, p. 1–12.
[7] Hussein MI, Leamy MJ, Ruzzene M. Dynamics of phononic materials and structures: Historical origins, recent progress, and future outlook. Appl Mech Rev 2014;66(4):040802.
[8] Chen Y, Qian F, Scarpa F, Zuo L, Zhuang X. Harnessing multi-layered soil to design seismic metamaterials with ultralow frequency band gaps. Mater Des 2019;175:107813.
[9] Finocchio G, Casablanca O, Ricciardi G, Alibrandi U, Garesci F, Chiappini M, et al. Seismic metamaterials based on isochronous mechanical oscillators. Appl Phys Lett 2014;104. 191903–191903.
[10] Achaoui Y, Antonakakis T, Brûlé S, Craster RV, Enoch S, Guenneau S. Clamped seismic metamaterials: Ultra-low frequency stop bands. New J Phys 2017;19(6):063022.
[11] Li T, Su Q, Kaewunruen S. Seismic metamaterial barriers for ground vibration mitigation in railways considering the train-track-soil dynamic interactions. Constr Build Mater 2020;260:119936.
[12] Albino C, Godinho L, Amado-Mendes P, Alves-Costa P, da Costa DD, Soares D. 3D FEM analysis of the effect of buried phononic crystal barriers on vibration mitigation. Eng Struct 2019;196:109340.
[13] Ouakka S, Verlinden O, Kouroussis G. Railway vibration mitigation measures: A case study based on the T2000 tram circulating in Brussels. In: 3rd international conference on natural hazards & infrastructure. Athens, Greece; 2022.
[14] Ouakka S, Verlinden O, Kouroussis G. Using natural seismic metamaterials to mitigate railway ground-borne vibration. In: International congress on sound and vibration. 2022.
[15] Kaewunruen S, Qin Z. Sustainability of vibration mitigation methods using meta-materials/structures along railway corridors exposed to adverse weather conditions. Sustainability 2020;12:10236.
[16] Kouroussis G, Verlinden O, Conti C. A two–step time simulation of ground vibrations induced by the railway traffic. J Mech Eng Sci 2012;226(2):454–72.
[17] Huang X, Lai Y, Hang ZH, Zheng H, Chan CT. Dirac cones induced by accidental degeneracy in photonic crystals and zero-refractive-index materials. Nature Mater 2011;10(8):582–6.
[18] Wu X, Wen Z, Jin Y, Rabczuk T, Zhuang X, Djafari-Rouhani B. Broadband Rayleigh wave attenuation by gradient metamaterials. Int J Mech Sci 2021;205:106592.
[19] Kittel C. Introduction to solid state physics. 5th ed.. vol. 21, New York: Wiley; 1996.
[20] Pu X, Shi Z. A novel method for identifying surface waves in periodic structures. Soil Dyn Earthq Eng 2017;98:67–71.
[21] Olivier B, Connolly DP, Costa PA, Kouroussis G. The effect of embankment on high speed rail ground vibrations. Int J Rail Transp 2016;4(4):229–46.
[22] Verlinden O, Ben Fekih L, Kouroussis G. Symbolic generation of the kinematics of multibody systems in EasyDyn: from MuPAD to Xcas/Giac. Theoretical & Applied Mechanics Letters 2013;3(1):013012.
[23] Degrande G, Roeck GD, Dewulf W, den Broeck PV, Verlinden M. Design of a vibration isolating screen. In: Sas P, editor. In: Proceedings ISMA 21, noise and vibration engineering, Vol. II, Leuven, Belgium; 1996, p. 823–34.
[24] Bettess P. Infinite elements. Sunderland, UK: Penshaw Press; 1992.
[25] Kouroussis G, Florentin J, Verlinden O. Ground vibrations induced by intercity/interregion trains: a numerical prediction based on the multi-body/finite element modeling approach. Journal of Vibration and Control 2016;22(20):4192–210.
[26] Kouroussis G, Van Parys L, Conti C, Verlinden O. Using three-dimensional finite element analysis in time domain to model railway–induced ground vibrations. Advances in Engineering Software 2014;70:63–76.
[27] Kouroussis G, Verlinden O, Conti C. Efficiency of resilient wheels on the alleviation of railway ground vibrations. Proc Inst Mech Eng 2012;226(4):381–96.
[28] Kouroussis G, Verlinden O, Conti C. On the interest of integrating vehicle dynamics for the ground propagation of vibrations: The case of urban railway traffic. Veh Syst Dyn 2010;48(12):1553–71.
[29] Khelif A, Achaoui Y, Benchabane S, Laude V, Aoubiza B. Locally resonant surface acoustic wave band gaps in a two-dimensional phononic crystal of pillars on a surface. Phys Rev B 2010;81:214303.